2016 IEEE 55th Conference on Decision and Control (CDC)
ARIA Resort & Casino
December 12-14, 2016, Las Vegas, USA

Synthesis of an Energy-Optimal Self-Heating Strategy for Li-ion Batteries

Shankar Mohan, Jason Siegel, Anna G. Stefanopoulou, Matthew Castanier and Yi Ding

***Abstract*— The resistance of Lithium-ion cells increases at sub-zero temperatures reducing the cells' power availability. One way to improve the cells' performance in these adverse operation conditions is to proactively heat them. In this paper, we consider the scenario in which a cell is heated from both inside and outside; a current is drawn from the cell to power a convective heater; Joule heating warms the cell from inside. A problem formulation to derive the time-limited energy-optimal current policy is presented, analyzed and numerically solved. It is observed that the optimal current policy resembles a sequence of constant voltage, constant current and phases, mirroring conventional wisdom. Finally, the notion of *productive warm-up*—a warm-up procedure that ensures that the cell can perform work once warmed-up—is introduced; and an approximation of the optimal solution is used to identify the lowest state of charge at various operating conditions (portion of the state-space) from which *productive warm-up* is feasible.**

I. Introduction

The importance of energy storage does not need introduction. Lithium-ion (Li-ion) batteries, having been in commercial production for about 25 years, have come to the forefront as primary energy-storage medium in non-stationary applications owing to their energy/power density. In practice, these batteries suffer from decreased efficiency, higher resistance and lower power-capability when operating in cold weather (less than zero degree Celsius). The range of electric vehicles can be reduced by 40% in cold weather [1].

Earlier methods to improve the low temperature performance of electrochemical energy systems have relied on engineering the materials that constitute the cell, to suppress the limiting processes [2], and on the design of heating methods that raise the operating temperature of the cell to favorable levels [3]–[8]. The authors of [3] compute and compare the energy requirement to warm NiMH battery packs using both internal and external heating techniques. Stuart *et. al.* in [4] present a method of battery warm-up that uses AC currents to effect internal heating. In [8], the notion of energy-efficient warm-up was introduced, a receding horizon based controller was designed to shuttle energy between the battery pack and ultracapacitor pack, and aimed to improve the power capability of Li-ion cells until a pre-specified power threshold was reached using internal heating. Muller *et. al.* in [5] present an optimal method to simultaneously warm-up a fuel cell whilst meeting power constraints. The authors in [6] compare a variety of warm-up techniques and conclude that internal warm-up is the most *efficient*. Wang *et. al.* in [7] present a novel battery design that incorporates a Nickel foil of a measured resistance inside a Li-ion cell for accelerated warm-up; before providing power to external loads, this foil is connected across the terminals and serves as a low resistance load.

In this paper, we consider the warm-up of Li-ion batteries in the presence of an external heater, until the batteries' temperature reaches a preassigned value. Particularly, we investigate the feasibility of energy-optimal warm-up of batteries. The external heater is powered by the battery pack and transfers heat energy to the battery via a medium such as air; that is, the battery is heated from inside by Joule heating (generated by the battery's own internal resistance) and from outside via convection. This process is assisted by a fan that maintains circulation inside the battery chamber; Fig. 1 presents a schematic of the system under consideration.

Since battery warm-up is inherently a process that depletes the battery's SOC, it is critical that any supervisory controller that regulates SOC be cognizant of the minimum required energy for warm-up. With this information, the supervisory controller that controls the power out-flow from the battery can ensure that warm-up of a cold battery is feasible. To the best of our knowledge, a systematic effort to certify the (in)feasibility of *productive warm-up*—a warm-up methodology that ensures that adequate energy remains post warm-up—has not been undertaken in literature. In this paper, we leverage our observations about the energy-optimal policy, and use its approximation to partition the state-space into regions based on whether warm-up is possible.

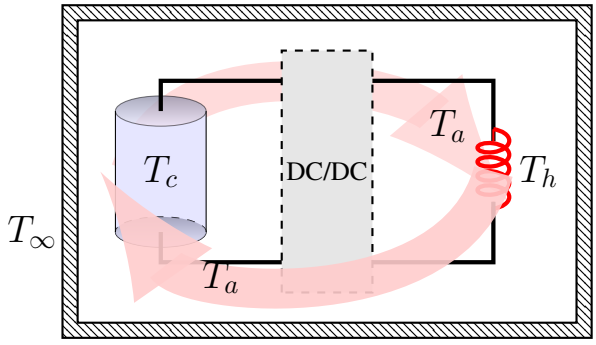

Fig. 1. A schematic of the system under consideration with annotations of the temperatures of the different elements under consideration

S. Mohan is with the Department of Electrical Engineering and Computer Science, University of Michigan, Ann Arbor, MI 48109 elemsn@umich.edu

A.G. Stefanopoulou & J. Siegel are with the Department of Mechanical Engineering, University of Michigan, Ann Arbor, MI 48109 {annastef,siegeljb}@umich.edu

M. Castanier & Y. Ding are with the United States Army Tank Automotive Research, Development and Engineering Center, Warren, MI {matthew.p.castanier.civ, yi.ding8.civ}@mail.mil

This paper is organized as follows: Section II presents the models used in this study, and the formulation of the optimal control problem (OCP) considered in the remainder of this paper. Section III presents an analysis of the optimal control and identifies a characteristic of the optimal solution. In addition, a methodology to numerically solve the OCP is presented and an example is solved and the solution is interpreted. Lastly, Section V summarizes observations/results and presents directions for future extensions alongside conclusions.

II. Preliminaries

In this section, the model of the system whose schematic is presented in Fig. 1 is detailed; subsequently, the optimal control problem whose solution is the energy-optimal policy for warm-up is presented.

A. System Modelling

The dynamics of the $LiFePO_4$ (A123 26650) battery in consideration hereafter is represented by a coupled electro-thermal model and is described in the following.

1) Electrical dynamics: The representation of the electrical sub-system of the battery whose capacity is Q_b Ahrs, is constituted by two states — one that corresponds to the State of Charge (z) and the other corresponding to bulk polarization voltage (v) across a virtual capacitor with capacitance C F.

$$\begin{aligned} \dot{z} &= -\frac{I}{3600 \cdot Q_b} \\ \dot{v}_c &= -\frac{v}{\tau(T_c)} + \frac{I}{C(T_c)} \\ v_t &= v_{oc}(z) - v_c - I \cdot R_s(T_c), \end{aligned} \tag{1}$$

where I is the current in Amperes (positive when discharging), temperature dependent real functions τ, C, R_s represent the time constant of the overpotential and ohmic drop respectively, and T_c is the battery's temperature. A polynomial approximation of these functions, derived from the data presented in [8], is presented in Eqns. (2).

2) Thermal dynamics: In this work, we assume that the battery is placed inside a chamber that has a re-circulation system built-in (refer Fig. 1). Further, a heater is located in the return path of circulated air; this heater is powered by the battery through a power electronic converter. The thermal dynamics of the cylindrical cell is modeled by a single state representing the bulk temperature (T_c) of the cell [9].

Parameter	α_1	α_2	α_3	β_1
Value	0.0214	0.0035	-0.0029	0.2331
Parameter	β_2	γ_1	γ_2	γ_3
Value	-0.1166	-4.6913	-7.1073	variable

TABLE I
PARAMETERS OF THE THERMAL MODEL

The coupled dynamics of all elements in the thermal loop is given by the following

$$\begin{aligned} \dot{T}_c &= \alpha_1 \cdot P_{Joule} + \alpha_2 \cdot T_a + \alpha_3 \cdot T_c, \\ \dot{T}_h &= \beta_1 \cdot P_{heater} + \beta_2 \cdot (T_a - T_h), \\ \dot{T}_a &= \gamma_1 \cdot (T_c - T_a) + \gamma_2 \cdot (T_h - T_a) - \gamma_3 \cdot (T_\infty - T_a), \end{aligned} \tag{2}$$

where T_∞, T_a, T_c, T_h are the temperatures of the atmosphere, air inside the chamber, cell, and the heater respectively; the values of the different parameters are as listed in Tab. I; and

$$P_{Joule} = I^2 \cdot R_s(T_c) + v_c^2 \frac{C(T_c)}{\tau(T_c)}, \; P_{heater} = \quad v_t \cdot I \tag{3a}$$

Observe that in the model under consideration, the ambient/atmospheric temperature, affects the dynamics of only the air inside the chamber. The material of the encasement affects the conductive losses between T_a and T_∞, and is a parameter whose influence on solutions will be studied in the ensuing presentation. It should be noted that despite assuming that a fan is present in the thermal loop—to enable better convective transfer of heat—the power delivered to the same is not explicitly modeled and is assumed to be insignificant.

B. The optimal control problem

The objective of this paper is to determine an energy-optimal warm-up (to a pre-specified temperature) strategy for batteries from sub-zero temperatures, without violating operating constraints. In the ensuing presentation, the mathematical formulation of the problem considered in the remainder of this paper is presented.

$$(OCP) \; \min z(t_f) - z(t_0) \tag{4}$$
$$\text{st. } Eqns.\ (1) - (3), \tag{5}$$
$$I(t) \in [0,\, I_{max}], \qquad \forall t \in [0,\, t_f] \tag{6}$$
$$v_t(t) \in [v_{min},\, v_{max}], \qquad \forall t \in [0,\, t_f] \tag{7}$$
$$T_c(t) \in [T_{min}, T^c_{max}], \qquad \forall t \in [0,\, t_f] \tag{8}$$
$$T_h(t), T_a(t) \in [T_{min}, T_{max}], \quad \forall t \in [0,\, t_f] \tag{9}$$
$$x(t_0) = x_0, \tag{10}$$
$$T_c(t_f) = T_{des}, \tag{11}$$
$$t_f = t_{max}, \tag{12}$$

$$\begin{aligned} R_s(T_c) &= -6.833 \times 10^{-7} T_c^3 + 5.477 \times 10^{-5} T_c^2 - 1.468 \times 10^{-3} T_c + 0.02421 \\ \tau(T_c) &= 1.088 \times 10^{-5} T_c^4 - 6.002 \times 10^{-4} T_c^3 - 1.961 \times 10^{-3} T_c^2 - 0.116 T_c + 47.57 \\ C(T_c) &= -1.186 \times 10^{-3} T_c^3 - 0.144 T_c^2 + 45.63 T_c + 1360 \\ v_{oc}(z) &= 1.528 z^3 - 2.264 z^2 + 1.193 + 3.091 \\ v_{min} &= 2 \text{ V}, Q = 2.3 \text{ Ah}, T^c_{max} = 35 \text{ °C}, T_{min} = -20 \text{ °C}, T_{max} = 150 \text{ °C}, I_{max} = 25 \text{ A}, v_{max} = 3.6 \text{ V}; \end{aligned} \tag{2}$$

where $x = [z,\, v_1,\, T_c,\, T_h,\, T_a]'$; T_{des} is the desired cell temperature set-point; I_{max} is the maximum discharge current; and v_{min} and v_{max} are the minimum and maximum terminal voltages of the battery.

In this paper, energy is measured in terms of SOC, and hence the objective function in Eqn. (4) represents the energy expended over the period $[0, t_f]$, where t_f is the maximum time for warm-up (or the longest that the user would like to wait) as defined by the constraint in Eqn. (12). Equations (6) & (7) enforce constraints on the current and voltage as specified by the battery manufacturer. Observe that in this case, the current is stipulated to be discharging in nature due to the lack of an external energy source. Additionally, the temperatures of the battery, heater and the air inside the chamber are restricted in the interest of safety as depicted in Eqns. (9). Finally, the constraint in Eqn. (11) enforces, as required, a terminal state constraint on the battery temperature.

III. Analysis and numerical solution

In this section, the optimal control problem (OCP) is analyzed to identify characteristics of the optimal policy. Subsequently, the problem is numerically solved for an example and the results are interpreted.

A. Analysis

To analyze the problem (OCP), we consider the Hamiltonian of (OCP) and arrive at the following result that asserts the control policy will at worst look like sequence of pulses.

Proposition 1. *The optimal current trajectory takes an extreme value of the admissible set at every instant.*

Proof (Sketch). The proof is laid-out as follows: it is argued that the Hamiltonian of this problem is concave in the decision variable – I. Recall that the optimal control at every instant minimizes the Hamiltonian with respect to I. Since the Hamiltonian will be shown to be concave in I, it follows that the optimal solution at each instant attains only extreme values of the admissible set.

Let the Hamiltonian of (OCP) be defined as follows:

$$H_T = \sum_{i=1}^{5} \psi_i f_i(x) + \sum_{i=1}^{5} \psi_i g_i(x) I + \sum_{i=1}^{5} \psi_i h_i(x) I^2 \quad (13)$$

where ψ_i are co-states and functions f_i, h_i are representations of the coefficients of the different monomials in I derived by simplifying the dynamics of the system whose dynamics is described by Eqns. (1)–(2); their values are presented in Tab. II.

Functions f, h and ψ are indexed to match the definition of x; that is, ψ_1 is the co-state corresponding to z and ψ_3 corresponds to T_c. Since H_T is quadratic in I, if $\sum_i \psi_i h_i$ is strictly negative, it would imply that H_T concave in I.

Using the entries in Tab. II, the coefficient of I^2 evaluates to

$$\kappa := \sum_i \psi_i h_i = \psi_3 \alpha_1 R_s(T_c) - \psi_4 \beta_1 R_s(T_c). \quad (14)$$

We know that, if V^* is the value function of (OCP), then [10, §3.5]

$$\psi_3(t) = \frac{\partial V^*(t)}{\partial T_c(t)}. \quad (15)$$

The objective of the OCP is to increase the temperature until $T_c = T_{des}$; if T_c increases, all other states remaining the same, the cost to go decreases as the T_c is closer to the target temperature. That is, ψ_3 is negative definite.

Now, since the numerical value of ψ_4 is not known, it is not possible to determine the sign of κ directly. We adopt an alternate approach: we define a virtual source sink for power, $\mathbf{S}$, and a virtual power source $\mathbf{P}$. Suppose the battery did not power the heater but sank power into $\mathbf{S}$; and that the heater is powered by $\mathbf{P}$ with a trajectory ζ. For the OCP with this new system, let the Hamiltonian be $\bar{H}_T$ and the costates be $\bar{\psi}_i$. The coefficient of I^2 in $\bar{H}_T$ is $\bar{\psi}_3 \alpha_1 R_s(T_c)$. That is, $\bar{H}_T$ is concave in I since $\bar{\psi}_3$ is negative definite, as established earlier.

Notice that the above argument is true regardless of the trajectory ζ that powers the heater. Suppose this ζ was identical to the power that was sank into $\mathbf{S}$. The new system becomes identical to the original system wherein the battery powered the heater. Thus the optimal solutions to the problems with Hamiltonians H_T and $\bar{H}_T$ are the same. Since $\bar{H}_T$ is concave in I, and the control set is convex, it follows that the optimal control policy to (OCP) will, at each time instance, attain an extreme admissible value. □

As a consequence of the above result, a possible optimal policy is the function $\hat{I} \mapsto \min\left\{I_{max}, \frac{v_{oc}(z(t)) - v_1(t) - v_{min}}{R_s(T_c(t))}\right\}$. When $\hat{I}(t) = I_{max}$, the battery is said to be operating in constant current mode; when $\hat{I}$ takes the other extreme value, the battery is said to be operating in the constant voltage mode ($v_t = v_{min}$).

TABLE II
List of placeholders in Eqn. (13) and the values/expressions they represent.

Variable	Expression/Value	Variable	Expression/Value	Variable	Expression/Value
f_1	0	g_1	$\frac{-1}{Q \cdot 3600}$	h_1	0
f_2	$\frac{-v_1}{\tau(T_c)}$	g_2	$\frac{1}{C_1(T_c)}$	h_2	0
f_3	$\alpha_1 v_1^2 \frac{C_1(T_c)}{\tau(T_c)} + \alpha_2 T_a + \alpha_3 T_c$	g_3	0	h_3	$\alpha_1 R_s(T_c)$
f_4	$\beta_2(T_a - T_h)$	g_4	$\eta(v_{oc}(z) - v_1)$	h_4	$-\eta R_s(T_c)$
f_5	$\gamma_1(T_c - T_a) + \gamma_2(T_h - T_a) - \gamma_3(T_\infty - T_a)$	g_5	0	h_5	0

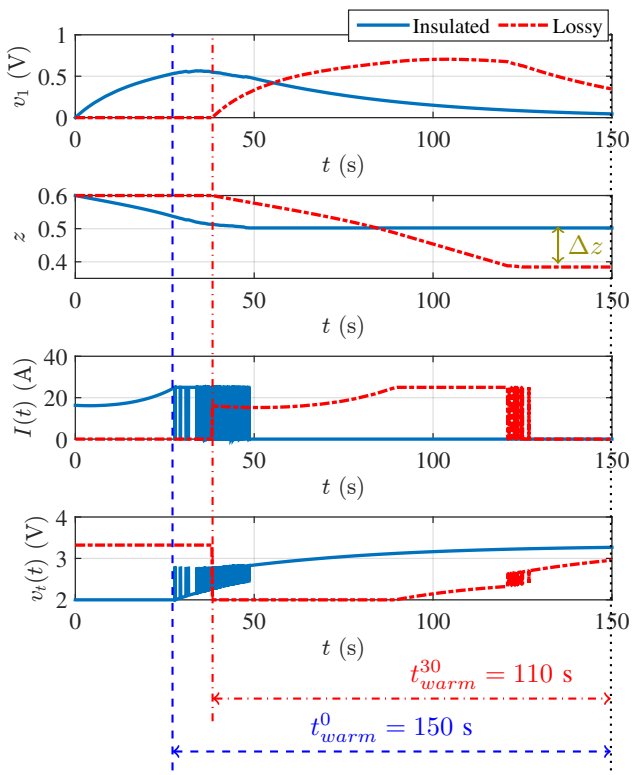

Fig. 2. Trajectories of states and output of the electrical subsystem as a consequence of applying the optimal policy; insulated ($\gamma_3 = 0$), lossy ($\gamma_3 = 30$). Observe that the optimal policy has three distinct phases – constant voltage, constant current and rest.

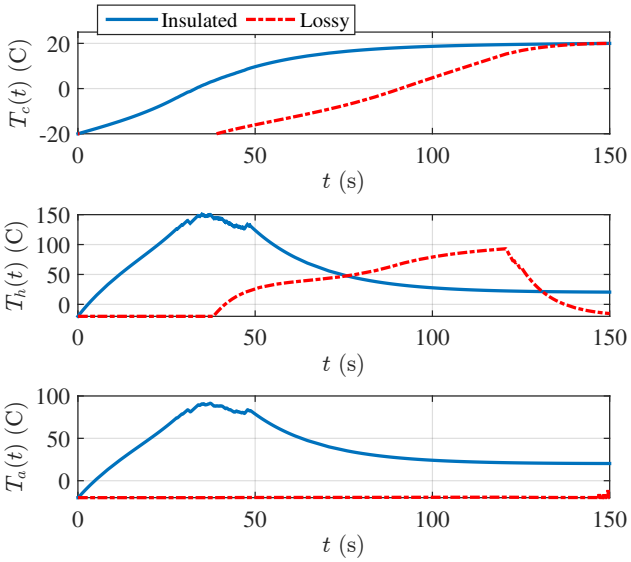

Fig. 3. Trajectories of states and output of the thermal subsystem as a consequence of applying the optimal policy; insulated ($\gamma_3 = 0$), lossy ($\gamma_3 = 30$)

B. Numerical solution

In this section, the optimal control problem (OCP) presented in Sec. II-B is numerically solved for some feasible initial system configuration. The OCP under consideration is nonlinear in dynamics (parameters are non-linear functions of temperature) and constraints (terminal voltage is a nonlinear function of SOC) and are not amenable to solve analytically. Additionally, since the dynamics has five states and one control, the use of Dynamic Programming approach is not computationally tractable.

In Sec. III-A it was shown that the optimal solution to the optimal control attains only extreme values at any instant. That is, the at any instance, the optimal warm-up policy forces the battery to operate either in one of the constant voltage (CV), constant current (CC) and rest phases. To leverage this information when solving the OCP, it is possible to hybridize the dynamics of the system based on the mode of operation and solve for the optimal switching sequence. Methods to solve hybrid nonlinear optimal control problem have been explored in literature; they are hard to implement and may not be suitable for problems of large dimensions due to their computational complexity [11], [12].

In this section, we use pseudo-spectral collocation to solve the OCPs (non-hybridized) using an off-the-shelf solver (IPOPT) using GPOPS2 as the problem parser [13].

Example 2. *Determine the optimal trajectory of current that consumes the least energy (in SOC) and is capable of increasing the battery's temperature (in thermal equilibrium with the air/heater/atmosphere and initial SOC,* 0.6*) from* -20 *°C to* 20 *°C within* 150 *s such that the SOC after warm-up is greater than* 0.35*.*

Figures 2 and 3 provide the results of solving and simulating the model for this example when the values of $\gamma_3 \in \{0, 30\}$. Recall that when γ_3 increases, the losses to the atmosphere increases; i.e. when $\gamma_3 = 0$, the battery enclosure is insulated from the atmosphere and when $\gamma_3 = 30$, the enclosure is a medium through which heat is lost to the atmosphere. Other constraints are set as provided in Eqn. (2). From Fig. 2, it is noted that the optimal current attains, at each instant, one of either the maximum or minimum admissible current. This results in the solution resembling a sequence of constant voltage (CV), constant current (CC) and rest phases.

The observed rest phase can be justified as follows. Working backwards from the terminal time, the rest phase that is observed is thought to be in place to exploit the built-up polarization inside the battery. Recall that the expression for heat generation includes the term v_c^2/R_1; when the value of heat generated in the R-C pair exceeds that of the heat lost to air, the optimal decision is to set $I = 0$.

The switching pattern observed in the optimal current can be explained in three ways – (1) the high frequency switching serves as a PWM sequence that essentially regulates the root-mean-square current to a certain value that is not an extreme point of the set of admissible control values without taking that value explicitly; (2) the size of mesh intervals and/or the tolerance of the solver is not adequately tight; (3) some state constraint is being violated. Based on the analysis presented earlier in this section, it is suggested that possibility (1) can be ruled-out. In Fig. 2, when the $\gamma_3 = 0$,

the heater's temperature T_h reaches a maximum of $\sim 150^\circ$ C, the boundary of the state constraint; by comparing Figs. 2 and 3 around the time when the heater temperature hits its constraint, it is indeed noted that the switching behavior is pronounced. Thus, it is suggested that the switching observed in the trajectory of current corresponding to the case when $\gamma_3 = 30$ (lossy) is not because of any state constraint being violated, and could be an artifice of the numerical method employed.

Figures 2 and 3 also highlight the influence of losses to the atmosphere through conduction losses. If the air-path is perfectly insulated ($\gamma_3 = 0$), then the optimal solution includes a rest phase following what appears to be CV-CC phases until the polarization voltage reduces to zero and the heater, air and cell are at thermal equilibrium at the desired temperature. On the other hand, if the air return path is made of a relatively highly conductive material such as aluminium, then the heat generated in the heater and transferred to air is wicked by the cold-air outside and the heating mechanism becomes ineffective. This particular case devolves into the standalone warm-up case discussed in [8].

In Fig. 2, the duration of warm-up, $t^{\gamma_3}_{warm}$—defined as the time duration between the first instance when current is drawn and 150 s—when the loss coefficient is γ_3, is shown for the two values of γ_3. Comparing the resultant trajectories for the two values of γ_3, observe that t^{30}_{warm} is shorter than t^{0}_{warm}, and that the rest phases following the CC phase is shorter when $\gamma_3 = 30$. The observation about the rest phase can be explained by recalling the previous discussion on the net heat generation in the cell being zero at $t = 150$ s; this can also be used to explain the rest before the CV phase. Secondly, observe that as a consequence of an increase in the value of γ_3, the SOC lost during warm-up increases by 11% (true), and the terminal SOC now is 39%; i.e. increased conduction losses increases the energy consumed during warm-up, as is to be expected.

To highlight the influence of conductive losses, Fig. 4 collates key metrics that can be used to study their influence on loss in SOC during warm-up and warm-up time $t^{\gamma_3}_{warm}$. Note that as γ_3 increases, the total loss in SOC (read as energy) during warm-up increases to reach an asymptote. Associated with this increasing value of γ_3, the duration of warm-up decreases; this observation is in line with our expectation as elucidated in the preceding discussion on the rest phase.

IV. Feasibility of productive warm-up

Serving as a power source, a battery is an energy storage device; and battery warm-up consumes energy (measured in SOC in this paper). If the battery is able to perform work after warm-up; i.e. if there is adequate energy remaining, the warm-up is deemed as having been *productive*. Suppose the minimum energy required at the end of warm-up is z_{limit} and that $I^* : [0, t_f] \to [0, I_{max}]$ is an optimal solution to (OCP), and $z^* : [0, t_f] \to [0, 1]$ is the resulting optimal SOC trajectory; then determining the feasibility of *productive warm-up* is equivalent to checking the condition $z^*(t_f) \geq z_{limit}$. In this section, we exploit the observation that the optimal policy resembles a sequence of constant voltage, constant current and rest phases, to approximate the optimal solution and use this solution to ascertain when *productive warm-up* is feasible.

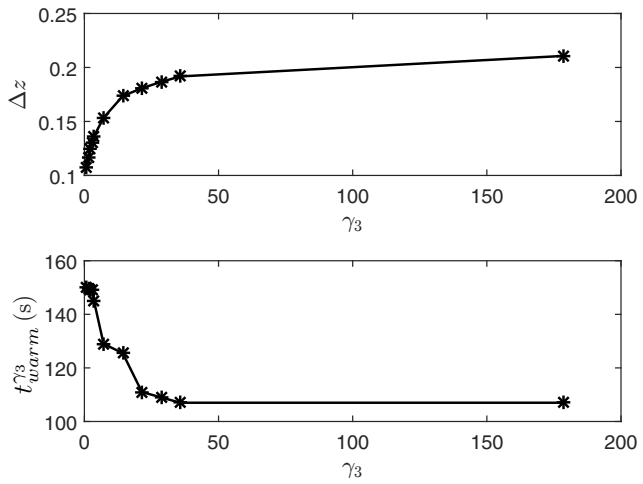

Fig. 4. Impact of changes to the value of γ_3 on the total SOC lost and the time for warm-up, T_{warm}. As the value of the loss coefficient increases, observe that the energy expended increases and the warm-up time decreases.

To estimate the feasible region of the state-space, we make two assumptions – (a) the battery is in thermal equilibrium with the atmosphere at the initial time; (b) the heat transfer coefficient is arbitrarily large. The first assumption is a physically realizable constraint that is satisfied, for example in resting electrified vehicles. As a consequence of this assumption, the initial value of v_1 is implicitly zero. The second assumption enforces that the air temperature inside the chamber is approximately equal to the atmosphere's temperature. With this assumption, as indicated in Sec. III-B, the heater does not contribute to battery warm-up; the states associated with chamber-air and heater temperatures can thus be ignored. It is easy to see that these assumptions help derive under-approximations of the feasible space.

To compute the under-approximation of the feasible space, the space $[-20, 20] \times [0.2, 0.7]$—corresponding to the space of initial battery temperature and SOC—is discretized into a 10×10 mesh and the dynamics is forward simulated by drawing the maximum admissible current at every instance, until the battery temperature reaches T_{des}. Figure 5 depicts the partition of the space given the specification that $T_{des} = 20$ °C and $z_{limit} = 0.35$. Observe that as the equilibrium temperature decreases, $\bar{T}$, the energy required to warm-up generally increases. However, as the values of $\bar{T}$ falls below ~ -15 °C, the required initial SOC decreases. This can be attributed to two factors – (1) increased internal resistance and lower temperatures that grows approximately exponentially; (2) the more significant role played by the heat generated by the polarization R-C pair.

As indicated, the feasible region identified in Fig. 5 is an under-approximation that is derived based on assumptions on

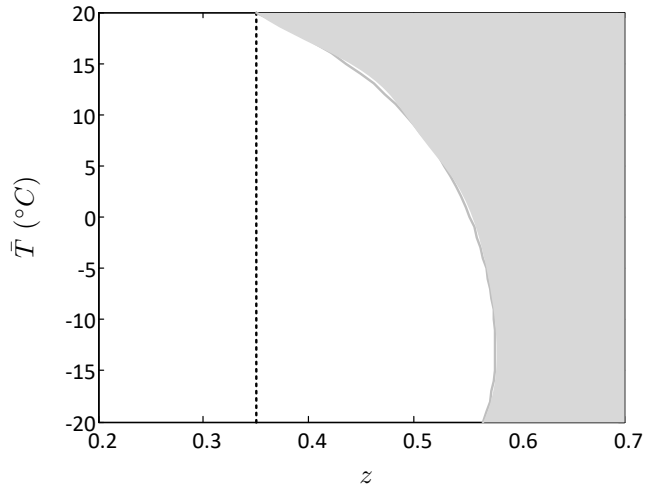

Fig. 5. Identification of the region of the space from which *productive* warm-up is feasible $z_{limit} = 0.35$. The gray region is the feasible space when the battery is initially in thermal equilibrium with the atmosphere at a temperature $\bar{T}$. In generating the above figure, the conduction coefficient γ_3 is assumed to be arbitrarily large.

the cooling condition and the shape of the control policy. To assess the conservativeness of the above map, an approximation of the feasible set will be computed using the method described in [14] and presented in a future work. Solving for the *productive warm-up* feasible space and storing it in memory, can be used for realtime adaptation of on-board supervisory controllers to steer the SOC of the battery such as to ensure that warm-up is possible.

V. Conclusions

In this paper, the problem of time-limited energy-optimal *productive warm-up* of Li-ion batteries from sub-zero temperatures when using a battery powered heater and convective heating is solved. A warm-up policy is deemed productive if it is capable of increasing the battery's temperature whilst ensuring that there is adequate energy stored to perform work after warm-up.

First, the temperature-driven energy-optimal control problem is analyzed and it is identified that the optimal solution, at every instant, attains only extreme values. Subsequently, the optimal control is solved and it is observed that the solution resembles a sequence of CV-CC-rest phases. The influence of losses to the atmosphere is investigated parametrically and it is noted that the system has to be reasonably well-insulated for the heater to be of any assistance in warm-up. Lastly, by approximating the optimal policy by a CV-CC sequence, the problem of ascertaining the feasibility of *productive warm-up* is addressed.

A future work will extend this work to account for uncertainties in model parameters (because of modeling errors and or because of aging) using the techniques presented in [15], and also consider terminating the warm-up using power capability based constraints, building upon the ideas presented in [8], [16].

Acknowledgements

The authors would like to acknowledge the technical and financial support of the Automotive Research Center (ARC) in accordance with Cooperative Agreement W56HZV-14-2-0001 U.S. Army Tank Automotive Research, Development and Engineering Center (TARDEC) in Warren, MI. UNCLASSIFIED: Distribution Statement A. Approved for public release; distribution is unlimited.

References

[1] Extreme temperatures affect electric vehicle driving range. http://newsroom.aaa.com/2014/03/extreme-temperatures-affect-electric-vehicle-driving-range-aaa-says, March 2014. Online. Accessed on 2/21/2016.

[2] S. Zhang, K. Xu, and T. Jow, "A new approach toward improved low temperature performance of Li-ion battery," *Electrochemistry Communications*, vol. 4, no. 11, pp. 928 – 932, 2002.

[3] A. Pesaran, A. Vlahinos, and T. Stuart, "Cooling and preheating of batteries in hybrid electric vehicles," in *The 6th ASME-JSME Thermal Engineering Joint Conference*, 2003.

[4] T. Stuart and A. Hande, "HEV battery heating using ac currents," *Journal of Power Sources*, vol. 129, no. 2, pp. 368 – 378, 2004.

[5] E. A. Muller, A. G. Stefanopoulou, and L. Guzzella, "Optimal power control of hybrid fuel cell systems for an accelerated system warm-up," *IEEE Transactions on Control Systems Technology*, vol. 15, pp. 290–305, March 2007.

[6] Y. Ji and C. Y. Wang, "Heating strategies for Li-ion batteries operated from subzero temperatures," *Electrochimica Acta*, vol. 107, pp. 664 – 674, 2013.

[7] C.-Y. Wang, G. Zhang, S. Ge, T. Xu, Y. Ji, X.-G. Yang, and Y. Leng, "Lithium-ion battery structure that self-heats at low temperatures," *Nature*, 2016.

[8] S. Mohan, Y. Kim, and A. G. Stefanopoulou, "Energy-conscious warm-up of li-ion cells from subzero temperatures," *IEEE Transactions on Industrial Electronics*, vol. 63, pp. 2954–2964, May 2016.

[9] X. Lin, H. E. Perez, S. Mohan, J. B. Siegel, A. G. Stefanopoulou, Y. Ding, and M. P. Castanier, "A lumped-parameter electro-thermal model for cylindrical batteries," *Journal of Power Sources*, vol. 257, pp. 1–11, 2014.

[10] G. C. Goodwin, M. M. Seron, and J. A. De Doná, *Constrained control and estimation: an optimisation approach*. Springer Science & Business Media, 2006.

[11] M. S. Shaikh and P. E. Caines, "On the hybrid optimal control problem: Theory and algorithms," *IEEE Transactions on Automatic Control*, vol. 52, pp. 1587–1603, Sept 2007.

[12] M. Claeys, J. Daafouz, and D. Henrion, "Modal occupation measures and {LMI} relaxations for nonlinear switched systems control," *Automatica*, vol. 64, pp. 143 – 154, 2016.

[13] M. A. Patterson and A. V. Rao, "GPOPS-II: A MATLAB software for solving multiple-phase optimal control problems using hp-adaptive gaussian quadrature collocation methods and sparse nonlinear programming," *ACM Transactions on Mathematical Software (TOMS)*, vol. 41, no. 1, p. 1, 2014.

[14] S. Mohan and R. Vasudevan, "Convex computation of the reachable set for hybrid systems with parametric uncertainty," in *2016 American Control Conference (ACC)*, pp. 5141–5147, July 2016.

[15] P. Holmes, S. Kousik, S. Mohan, and R. Vasudevan, "Convex Estimation of the α-level Reachable Sets of Systems with Parametric Uncertainty," in *2016 IEEE 55nd Annual Conference on Decision and Control (CDC)*, 2016.

[16] S. Mohan, Y. Kim, and A. G. Stefanopoulou, "Estimating the Power Capability of Li-ion Batteries Using Informationally Partitioned Estimators," *IEEE Transactions on Control Systems Technology*, vol. 24, pp. 1643–1654, Sept 2016.